ALCAM contributes to brain metastasis formation in non-small-cell lung cancer through interaction with the vascular endothelium

Justine Münsterberg,[†] Desirée Loreth,[†,◉] Laura Brylka, Stefan Werner, Jana Karbanova, Monja Gandrass, Svenja Schneegans,[◉] Katharina Besler, Fabienne Hamester, José Ramon Robador, Alexander Thomas Bauer, Stefan Werner Schneider, Michaela Wrage, Katrin Lamszus, Jakob Matschke, Yogesh Vashist, Güntac Uzunoglu, Stefan Steurer,[◉] Andrea Kristina Horst, Leticia Oliveira-Ferrer,[◉] Markus Glatzel, Thorsten Schinke, Denis Corbeil, Klaus Pantel,[◉] Cecile Maire, and Harriet Wikman,[◉]

Department of Tumor Biology, University Medical Center Hamburg-Eppendorf, Hamburg, Germany (J.M., D.L., S.W., M.G., S.S., K.B., M.W., K.P., H.W.); Department of Osteology and Biomechanics, University Medical Center Hamburg-Eppendorf, Hamburg, Germany (L.B., T.S.); Biotechnology Center and Center for Molecular and Cellular Bioengineering, Technical University Dresden, Dresden, Germany (J.K., D.C.); Department of Gynecology, University Medical Center Hamburg-Eppendorf, Hamburg, Germany (F.H., L.O-F.); Experimental Dermatology, Department of Dermatology, Venereology and Allergy, Medical Faculty Mannheim, University of Heidelberg, Mannheim, Germany (J.R.R., A.T.B.); Department of Dermatology and Venerology, University Hospital Hamburg-Eppendorf, Hamburg, Germany (J.R.R., A.T.B., S.W.S.); Department of Neurosurgery, University Medical Center Hamburg-Eppendorf, Hamburg, Germany (K.L., C.M.); Department of Neuropathology, University Medical Center Hamburg-Eppendorf, Hamburg, Germany (J.M., M.G.); General, Visceral and Thoracic Surgery Department, University Medical Center Hamburg-Eppendorf, Hamburg, Germany (Y.V., G.U.); Institute of Pathology, University Medical Center Hamburg-Eppendorf, Hamburg, Germany (S.S.); Institute for Experimental Immunology and Hepatology, University Medical Center Hamburg-Eppendorf, Hamburg, Germany (A.K.H.)

Corresponding Author: Harriet Wikman, Ph.D., Department of Tumor Biology, University Medical Center Hamburg-Eppendorf, Martinistraße 52, 20246 Hamburg, Germany (h.wikman@uke.de).

[†]Shared first authorship.

Abstract

Background. Brain metastasis (BM) in non-small-cell lung cancer (NSCLC) has a very poor prognosis. Recent studies have demonstrated the importance of cell adhesion molecules in tumor metastasis. The aim of our study was to investigate the role of activated leukocyte cell adhesion molecule (ALCAM) in BM formation in NSCLC.

Methods. Immunohistochemical analysis was performed on 143 NSCLC primary tumors and BM. A correlation between clinicopathological parameters and survival was developed. Biological properties of ALCAM were assessed in vitro by gene ablation using CRISPR/Cas9 technology in the NCI-H460 NSCLC cell line and in vivo by intracranial and intracardial cell injection of NCI-H460 cells in NMRI-*Foxn1*[nu/nu] mice.

Results. ALCAM expression was significantly upregulated in NSCLC brain metastasis ($P = 0.023$) with a de novo expression of ALCAM in 31.2% of BM. Moderate/strong ALCAM expression in both primary NSCLC and brain metastasis was associated with shortened survival. Functional analysis of an ALCAM knock-out (KO) cell line showed a significantly decreased cell adhesion capacity to human brain endothelial cells by 38% ($P = 0.045$). In vivo studies showed significantly lower tumor cell dissemination in mice injected with ALCAM-KO cells in both mouse models, and both the number and size of BM were significantly diminished in ALCAM depleted tumors.

Conclusions. Our findings suggest that elevated levels of ALCAM expression promote BM formation in NSCLC through increased tumor cell dissemination and interaction with the brain endothelial cells. Therefore, ALCAM could be targeted to reduce the occurrence of BM.

Key Points

1. ALCAM expression associates with poor prognosis and brain metastasis in NSCLC.

2. ALCAM mediates interaction of NSCLC tumor cells with brain vascular endothelium.

3. ALCAM might represent a novel preventive target to reduce the occurrence of BM in NSCLC.

Importance of the Study

Lung cancer patients with brain metastasis have a very poor prognosis. Recent studies have demonstrated the importance of cell adhesion molecules in the tumor cell dissemination and metastasis process. The brain is a unique site of metastasis, since it is protected by the blood–brain barrier. We have identified the expression of cell adhesion molecule ALCAM to be upregulated in BM of lung cancer patients, which is furthermore associated with poor outcome. Importantly, our results indicate that ALCAM is directly involved in brain metastasis formation by promoting adherence to the cerebrovascular endothelium. As ALCAM inhibition is currently being evaluated in an ongoing phase II study for treatment of solid tumors, future evaluation of ALCAM expression may better stratify patients for optimized treatment. Additionally, our study is the first showing that ALCAM contributes to brain metastasis formation in NSCLC and could be a potential therapeutic target.

Lung cancer is the most common cause of cancer-related death, accounting for about 27% of all cancer deaths.[1,2] Despite new treatment, the 5-year survival rate of non-small-cell lung cancer (NSCLC) remains only around 15% in developed countries, with most cases being diagnosed in advanced stages with very poor outcome.[3] Brain metastases (BM) are a frequent complication in lung cancer patients, presenting in approximately 40% of patients with advanced adenocarcinoma and 50% with small-cell lung cancer.[4,5] Around 10% of adenocarcinoma patients present with brain metastasis at the time of initial diagnosis[6] and in 50% the brain is the only site of tumor relapse (oligo-metastasis).[7] Patients with BM have a very poor prognosis, with a 5-year survival rate of 2.9% and a high burden of neurological symptoms.[8–10] One of the main problems for treatment of BM is the blood–brain barrier (BBB). The endothelial cells (ECs) of the BBB are nonfenestrated and reinforced by the basal membrane and the end-feet of astrocytes, tightly regulating the movement of molecules, ions, and cells across the BBB, thus creating a substantial barrier for drug delivery to the central nervous system.[11,12]

In the context of the "seed and soil" hypothesis, the successful colonization of brain metastatic cells depends on specific properties of tumor cells to both access and survive in the brain.[13,14] Circulating tumor cells (CTCs) are the seeds of metastases, and detection of CTCs in NSCLC patients negatively correlates with clinical outcome.[15]

Interestingly, we and others have shown that CTCs from brain metastatic patients commonly are negative for epithelial cell adhesion molecule and thus display mesenchymal and stem cell traits.[16,17] CTCs from breast cancer patients with BM were shown to commonly express cluster of differentiation 44 (CD44), a protein involved in cell-cell interactions and cell adhesion.[16] Different cell adhesion molecules (CAMs) have been shown to be involved in the process of metastasis. A deregulation of CAMs contributes to the detachment of cells from the primary mass leading to tumor progression and to metastasis to distant sites.[18,19] In breast cancer BM, L1CAM has been shown to mediate the vascular co-option of tumor cells to brain-related microvascular endothelium, thereby promoting BM formation.[20,21] Other CAMs have also been implicated to play an important role in BM formation of different tumor entities,[22] including activated leukocyte cell adhesion molecule (ALCAM) in early stages of breast cancer metastasis seeding to the brain and vascular CAM-1 promoting adhesion of prostate carcinoma cells to brain ECs.[23,24]

In this study, we investigated the role of ALCAM in NSCLC brain metastasis formation. Both primary NSCLC tumor tissue as well as brain metastatic tissue were investigated. ALCAM expression was found to be significantly associated with BM and thus its functional role was investigated in both in vitro and mouse models.

Materials and Methods

Patient Materials

Tissue microarrays of formalin-fixed, paraffin-embedded tissues including tissue from 51 primary lung tumors, 15 lymph node metastases, and 76 lung cancer BM were examined. Additionally, whole sections of 16 matched pairs of primary lung tumor tissue and corresponding BM were analyzed. Furthermore, serum ALCAM levels were measured in 120 NSCLC patients, including 62 early stage non-metastatic patients, 34 multi-metastatic patients, and 24 oligo-BM patients. All patients had undergone surgery of both primary tumor and BM at the University Medical Center Hamburg-Eppendorf between 1998 and 2015. Ethical approval for this study was granted by the institutional review board Ethical Review Board of Hamburg analyses of human materials (PV4954). See also Supplementary Material.

Immunohistochemistry

For immunohistochemistry, ALCAM antibody (1:400, Vector Laboratories, VP-C375) was visualized by the Dako REAL Detection System (Peroxidase/DAB+, K5001) according to manufacturer's protocol and counterstained with hematoxylin. See also Supplementary Material.

Detection of Circulating Tumor Cells

Thirty-seven metastatic NSCLC patients were screened for CTCs using a microfluidic device (Parsortix, Angle).[25] Collected in EDTA tubes was 7.5 mL of peripheral blood, which was processed immediately by the Parsortix device, followed by a cytocentrifugation of the obtained cells onto slides. The cells were visualized by immunofluorescence staining using antibodies against human keratins (1:100, clone AE1/AE3, eBioscience), ALCAM (1:150, clone 3A6, Biolegend), and CD45 (1:150; clone HI30, Biolegend). CTCs were defined as keratin+/4′,6′-diamidino-2-phenylindole positive (DAPI+)/CD45−. See also Supplementary Material.

ALCAM ELISA

A sandwich enzyme-linked immunosorbent assay (ELISA) was used to quantify peripheral blood serum levels of secreted ALCAM (sALCAM) using the DuoSet ELISA Development kit (R&D Systems, DY656) according to the manufacturer's protocol. The probes were analyzed in 96-well microtiter plates as duplicates using a microplate reader set to 450 nm (Infinite M200Pro, Tecan NanoQuant).

Generation of ALCAM-KO Cell Line

Human NCI-H460 (hereafter H460) was obtained from American Type Culture Collection. To establish ALCAM-KO cells, we used clustered regularly interspaced palindromic repeat (CRISPR)/CRISPR-associated nuclease 9 (Cas9) technology. Successful ALCAM-KO was verified by immunoblot analysis and Sanger sequencing of individual expanded cell clones. Finally, a pool of 5 individually expanded H460 ALCAM-KO cell clones was used for all further experiments. See also Supplementary Material.

Proliferation, Migration, and Colony Formation

Cellular proliferation was assessed by MTT assay. For migration, a Boyden-chamber assay was used and colony formation was evaluated in soft agar assays. Adhesion capacity on human ECs was evaluated by using a static adhesion test as well as under dynamic conditions. See also Supplementary Material.

Scanning Electron Microscopy

Parental and ALCAM-KO H460 cells were plated individually or as a mixture (1:1) with brain ECs (HBEC-5i) and grown on 0.5% gelatin-coated coverslips for 2 days. Thereafter, samples were fixed in 2% glutaraldehyde for 1 h at room temperature and then overnight at 4°C. Following a 16 h post-fixation in 1% OsO_4 at 4°C, they were dehydrated in an acetone gradient (25–100%) and critical point dried in a CO_2 system (Critical Point Dryer, Leica Microsystems, EM CPD 300). Samples were then sputter coated with gold (sputter coating device SCD 050, BAL-TEC) and examined at a 5-kV accelerating voltage in a field emission-scanning electron microscope (Jeol JSM 7500F).

Animal Experiments

All mice experiments were performed in accordance with the guidelines of animal welfare of the University Medical Center Hamburg-Eppendorf and the local authorities (the Social, Health, and Consumer Protection Agency, Hamburg, Germany). Mice were kept on a 12:12 light-to-dark cycle with ad libitum access to food and water.

Two different mouse models were used. Parental and ALCAM-KO H460 cells were injected either intracranially in the right striatum ($n = 5$ per group) or intracardially into the left ventricle ($n = 10$ per group) of 12-week-old female NMRI-$Foxn1^{nu/nu}$ mice, respectively. Based on pilot experiments, mice were sacrificed 10 days after intracranial injection or by reaching a weight loss of more than 10% after intracardial injection (between days 17 and 21). One mouse injected intracranially with H460 ALCAM-KO cells did not show any signs of a brain tumor, most likely due to a faulty injection, and was thus excluded from further analysis. Similarly, in the intracardial injection model, one mouse in each group was excluded due to probably failed injection and therefore no tumor formation. Blood was collected from the eye vein, bone marrow was isolated from the left femur and tibia, and whole brain and peripheral organs were paraffin embedded. Brain tumor growth was calculated as $V_t = (\sqrt{(max. cross - sectional\ area)})^3$ as described by Kunkel et al.[26] The metastases in the ventricles in the intracranial model were not considered for tumor volume calculation. CD34+ blood vessels were counted

as described in Kunkel et al.[26] In brief, blood vessels per cross-sectional area were counted in 10 high powered fields for intracranial injected tumors. As brain tumors induced through intracardial injection were smaller in size, blood vessels per total cross-sectional area were counted. Liquid biopsy analysis for CTC and disseminated tumor cell (DTC) number in mouse blood and bone marrow was performed and visualized by immunofluorescence staining for human pan-keratin (1:100, clone AE1/AE3, eBioscience) and mouse CD45 (1:150, clone 30-F11, BD Pharmingen). For automatic cell identification, the Xcyto Quantitative Cell Imager (Chemometec) was used.[27] Histology and micro–computed tomography (μCT) analyses of the spines and the right femora were performed as described in Supplementary Material.

Statistics

Data are presented as group averages ± standard deviation (SD) or median ± intraquartile range. Statistical analysis of patient samples was performed using SPSS 23.0. The correlation of clinical and pathological variables with the staining was examined using the chi-square test or Fisher's exact test. Kaplan–Meier survival curves were compared with the log-rank test. Statistical analysis of mice samples was performed using GraphPad Prism 8.0.

For simple comparison, Student's t-test or Mann–Whitney test was performed. $P < 0.05$ was accepted as significant.

Further information is provided in the Supplementary Material.

Results

ALCAM Protein Expression in NSCLC Primary Tumors and Metastases

Immunohistochemical staining was performed for ALCAM on tissue microarrays. ALCAM protein expression data were obtained from 47 primary tumors, 15 lymph node metastases, and 71 BM samples. ALCAM expression was significantly increased in BM compared with primary tumor tissue ($P = 0.023$; Fig. 1A–D) as well as in lymph node metastases compared with primary tumor tissue ($P = 0.041$). ALCAM expression was strong in 50.7% of BM compared with 46.6% of lymph node metastases and 27.7% of primary tumors. In order to evaluate the change in ALCAM expression from the primary tumor tissue to the brain metastatic tissue, 16 whole sections of matched pairs were analyzed—37.5% ($n = 6$) of the primary tumors showed no ALCAM expression, whereas only one specimen of the matched brain metastasis was negative for ALCAM, indicating a de novo expression of ALCAM in 31.2% of
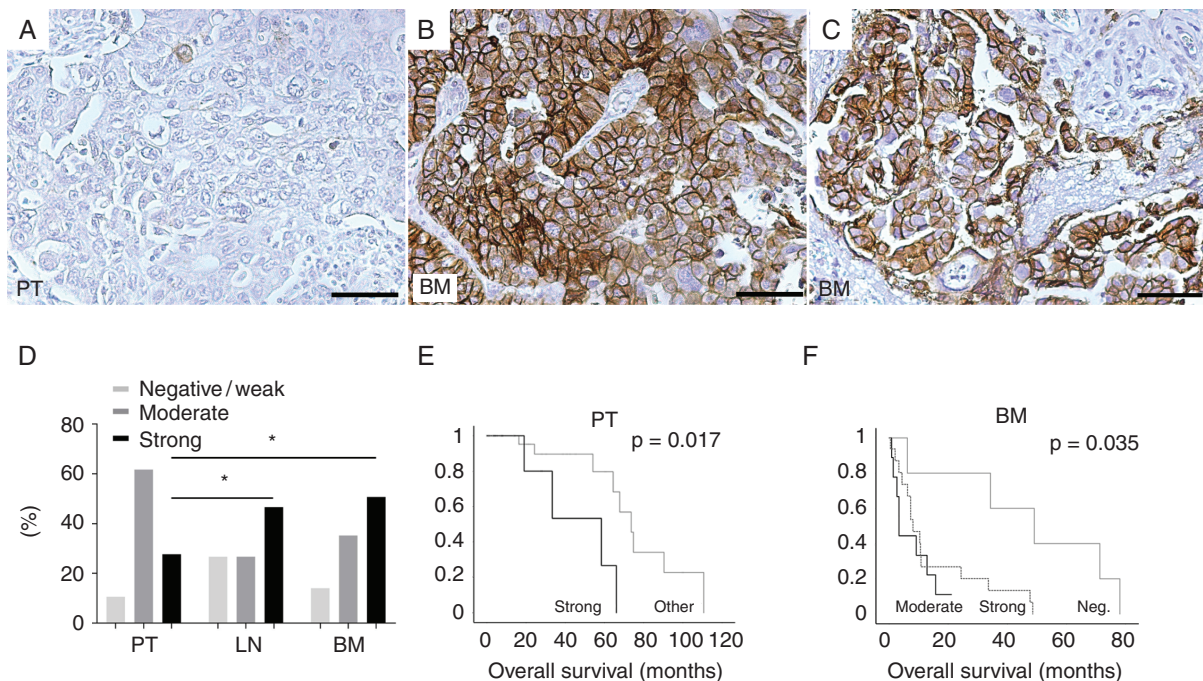
Fig. 1 ALCAM expression in primary tumor and metastatic tissue from NSCLC patients. ALCAM protein expression in (A) primary tumor (PT) and (B, C) 2 different BM from a NSCLC patient. (D) Frequency of ALCAM expression in PT, lymph node metastases (LN), and BM tissue (PT – BM $P = 0.023$, PT – LN $P = 0.04$). Survival analysis by Kaplan–Meier showing a significantly shortened OS for patients with positive ALCAM protein expression in (E, strong $n = 13$, other $n = 33$) NSCLC primary tumors and (F, moderate $n = 9$, strong $n = 16$, negative $n = 5$) NSCLC BM. The P-value was determined using the log-rank test. Scale bar 20 μm.

BM. In one patient, 2 BM diagnosed and operated one year apart showed very strong ALCAM expression in comparison to the negative primary tumor tissue (Fig. 1A–C). Additionally, 25% (*n* = 4) of samples showed an increase from moderate to strong ALCAM expression.

ALCAM Expression in Correlation with Clinicopathological Parameters and Prognosis

Correlation between the ALCAM protein expression pattern and clinicopathological parameters was assessed. A strong ALCAM expression in primary NSCLC tumors was only significantly correlated with a positive lymph node status (*P* = 0.019) (Table 1), whereas in brain metastatic tissue we found ALCAM to be correlated with both an oligo–brain metastatic status (brain as only site of metastasis, *P* = 0.046) as well as the presence of BM at initial diagnosis (*P* = 0.034). Survival analysis showed a correlation between ALCAM expression and overall survival (OS) in both primary tumors as well as BM samples. Patients with strong ALCAM expression in their primary tumors showed a significantly shortened OS compared with tumors with less ALCAM expression (*P* = 0.017; Fig. 1E). Likewise, a strong or moderate ALCAM expression in BM correlated with a shorter brain-specific OS (*P* = 0.035; Fig. 1F).

ALCAM Expression on Circulating Tumor Cells and Matched Brain Metastases

As we detected a de novo expression of ALCAM in a substantial number of BM, we investigated whether this de novo expression occurred during dissemination or rather during outgrowth of the metastasis in the brain. To this end, we analyzed the ALCAM expression on CTCs isolated by Parsortix (Fig. 2A) and matched BM (Fig. 2B). Keratin-positive CTCs were found in 4 out of 37 NSCLC patients with BM. In all these patients, we found congruent expression patterns of ALCAM on both CTCs and the matched BM tissue (Fig. 2C). Sadly no matching primary tumor tissue was available for these patients.

Secreted ALCAM in Plasma Levels of NSCLC Patients

ALCAM exists both as a transmembrane as well as a secreted protein (sALCAM).[28] To analyze if also sALCAM is associated with BM, sALCAM was quantified in peripheral blood plasma samples using a sandwich ELISA. One hundred twenty NSCLC patients with early-staged (*n* = 62), advanced multi metastatic (*n* = 34), or oligo-BM (*n* = 24) disease were analyzed. Levels of sALCAM were significantly elevated in the serum of multi-metastatic NSCLC patients (Fig. 2D, *n* = 34; mean 2338 pg/mL) compared with non-metastatic patients (*n* = 62; mean 1772 pg/mL; *P* = 0.001). The sALCAM serum levels of multi-metastatic NSCLC patients were also significantly elevated compared with oligo-BM patients (*n* = 24; mean 1700 pg/mL; *P* = 0.02). We defined the median sALCAM value as a cutoff value for the categorical analysis of sALCAM data in association with histopathological data.

An elevated sALCAM level showed a significant correlation neither with any histopathological data nor with patient survival, indicating that the cellular ALCAM is more important for BM formation than the secreted form.

In Vitro Model of ALCAM Function in NSCLC

To elucidate a role of ALCAM in the formation of BM in lung cancer, we established an in vitro model by using the NSCLC cell line NCI-H460. This cell line, derived from a pleural effusion of an NSCLC patient, has been shown to be able to metastasize to the brain and other organs.[21] Using CRISPR/Cas9 technology, a targeting plasmid for ALCAM inactivation was introduced in these cells and ALCAM absence was confirmed after cell expansion by immunoblot and immunofluorescence labeling (Fig. 3A, Supplementary Fig. 1A, B). Assays were performed to test whether the absence of ALCAM influenced basic cell functions. We observed no effect on proliferation (Fig. 3B), migration (Fig. 3C), and colony formation (Fig. 3D).

As ALCAM is an adhesion molecule, the effect of ALCAM inactivation on adhesion on different surfaces was assessed. A static adhesion assay in co-culture with brain ECs (hCMEC/D3) was performed. Fluorescence intensity of green fluorescent protein was measured after washing using Infinite M200 (Tecan). The adhesion of H460 ALCAM-KO cells to brain ECs was significantly decreased by 29% (*P* ≤ 0.001) compared with H460 parental cells (Fig. 3E). To further assess this interaction, adhesion under flow conditions, mimicking the blood stream in microvessels, was performed.[29] Adhesion of both parental and ALCAM-KO H460 cells is impaired under shear stress—however, to a different extent: 38% of H460 ALCAM-KO cells compared with 19% of H460 parental cells (*P* = 0.045) detached from the EC monolayer under shear stress (Fig. 3F), indicating that ALCAM plays a role in cell adhesion to brain ECs.

As the adhesion of ALCAM-KO cells on brain ECs was significantly decreased, we assessed the interaction more closely using a scanning electron microscope. When the cells were grown on gelatin, the H460 parental cells showed a more flattened shape and had numerous cell ruffles on the cell surface (Fig. 3G, H). In contrast, the ALCAM-KO cells showed a rounder shape, possibly indicating a lower attachment to the surface. Interestingly, the ALCAM-KO cells did not have many ruffles on the surface but instead displayed more microvilli (Fig. 3J, K). When grown together with human brain ECs, both the parental and ALCAM-KO cells interacted with the ECs. However, the contact was much more pronounced in the parental cells (Fig. 3M) compared with a contact via the microvilli in the ALCAM-KO cells (Fig. 3N). Immunofluorescence staining of CD9, a known interaction partner of ALCAM,[30,31] revealed localization to the membrane ruffles in parental cells, whereas it relocalized in microvillar-like structures in ALCAM-KO cells (Supplementary Fig. 1C–F).

In Vivo ALCAM Model

We injected the parental and ALCAM-KO H460 cells either intracranially or intracardially in nude mice to determine if inactivation of ALCAM affected tumor outgrowth in the

Table 1   ALCAM protein expression in correlation to clinical parameters in primary NSCLC and NSCLC brain metastasis

	total n	ALCAM			P
		negative + weak %	moderate %	strong %	value
Brain metastases					
Total	**71**	**14.1**	**35.2**	**50.7**	
Histology					n.s.
Adeno-CA	**54**	9.3	35.2	55.6	
SCC	**9**	22.2	33.3	44.4	
other	**5**	40.0	40.0	20.0	
Oligometastasis					0.046
no	**13**	30.8	38.5	30.8	
yes	**36**	5.6	38.8	55.6	
BM at diagnosis					0.034
no	**30**	20.0	43.3	36.7	
yes	**21**	0.0	33.3	66.7	
Oligo-BM at diagnosis					0.006
no	**30**	16.7	56.7	26.7	
yes	**18**	0.0	27.8	72.2	
Sex					n.s.
female	**27**	22.2	37.0	40.7	
male	**44**	9.1	34.1	56.8	
UICC stage					n.s.
I+II	**3**	66.7	0.0	33.3	
III+IV	**29**	13.8	37.9	48.3	
Primary tumors					
Total	**47**	**10.6**	**61.7**	**27.7**	
Histology					n.s.
Adeno-CA	**21**	9.5	71.4	20.0	
SCC	**17**	11.1	61.1	27.8	
Tumor stage					n.s.
pT1 + 2	**35**	8.6	62.9	28.6	
pT3 + 4	**12**	16.7	58.3	25.0	
Grade					n.s.
I+II	**24**	8.3	62.5	29.2	
III+IV	**23**	13.0	60.9	26.1	
Lymph node status					0.019
negative	**22**	9.1	81.8	9.1	
positive	**25**	12.0	44.0	44.0	
Metastasis					n.s.
M0	**43**	11.6	60.5	27.9	
M1	**4**	0.0	75.0	25.0	
UICC stage					n.s.
1 + 2	**27**	11.1	74.1	14.8	
3 + 4	**19**	10.5	47.4	42.1	
Age					n.s.
<63.1 y	**24**	16.7	58.3	25.0	
≥63.1 y	**23**	4.3	65.2	30.4	

Table 1 Continued

	total n	ALCAM			P
		negative + weak	moderate	strong	
		%	%	%	value
Sex					**n.s.**
female	**16**	18.8	50.0	31.3	
male	**31**	6.5	67.7	25.8	
Course of disease					**n.s.**
dead	**33**	9.1	63.6	27.3	
alive	**13**	15.4	53.8	30.8	

n.s. = not significant. SCC = squamous cell carcinoma. UICC = Union internationale contre le cancer.
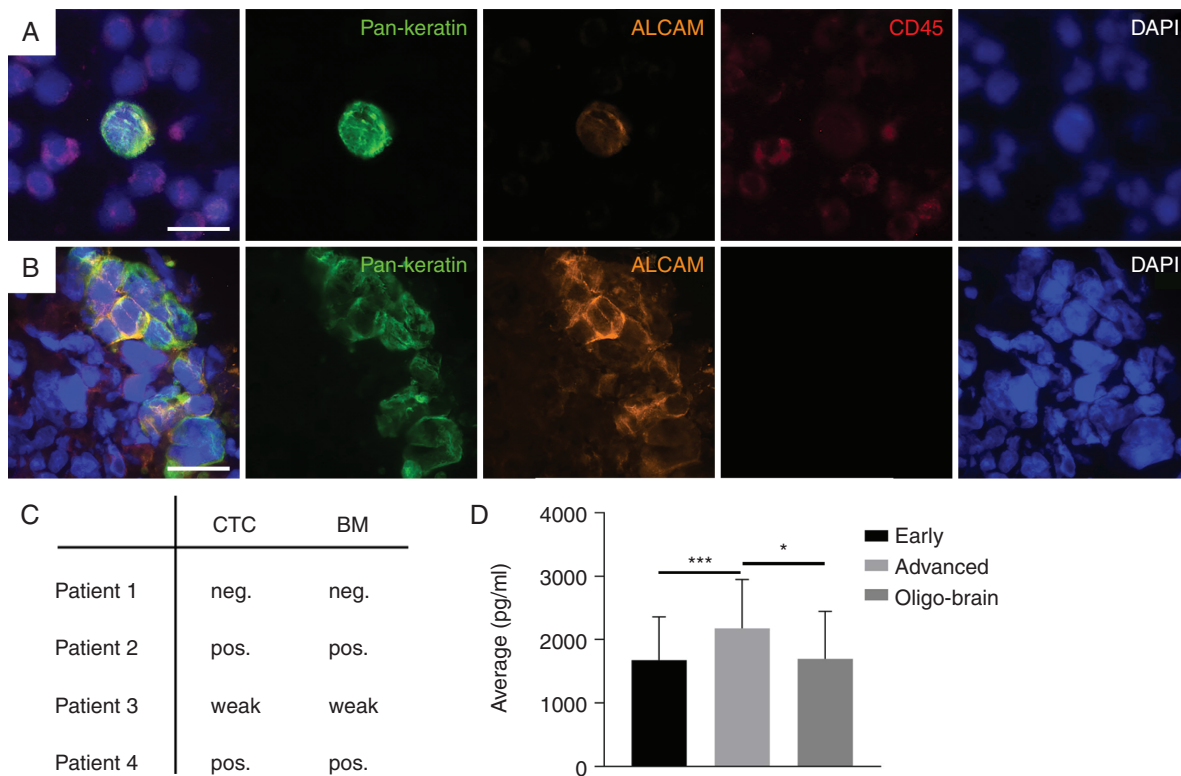
Fig. 2 ALCAM as BM marker in liquid biopsy. Immunofluorescent staining of ALCAM on a (A) CTC and matched (B) brain metastasis sample. (C) Correlation of ALCAM expression on CTCs with matched NSCLC brain metastasis tissue. (D) Secreted ALCAM serum analysis in non-metastatic (M0), oligo-BM and multisite metastatic NSCLC patients showing significantly elevated sALCAM level in advanced cancer patients compared with early staged patients ($P = 0.001$) and oligo-BM patients ($P = 0.02$). Mean ± SD. Scale bar 20 μm.

brain or dissemination. In the intracranial model, at time of sacrifice large tumors were detected in the brain but no overt tumors (serial sectioning) were seen outside the brain. However, a significant difference in the number of CTCs was detected. Twenty-nine CTCs per 1 million peripheral blood mononuclear cells (PBMCs) were found in mice injected with H460 parental cells, whereas no CTCs were found in the H460 ALCAM-KO injected mice (Fig. 4B). Similarly,

analysis for DTCs in the bone marrow revealed 44% fewer DTCs (20 DTCs per 1 million PBMCs) in H460 ALCAM-KO injected mice compared with H460 parental injected ones (36 DTCs per 1 million PBMCs) (Fig. 4E). Although the median size of brain tumors was lower in H460 ALCAM-KO injected animals, the difference did not reach significance (parental 140.1, range 80.2–237.1 mm³, ALCAM-KO 67, range 28.7–160.4 mm³, $P = 0.1905$; Fig. 5A, B, D). Interestingly, a
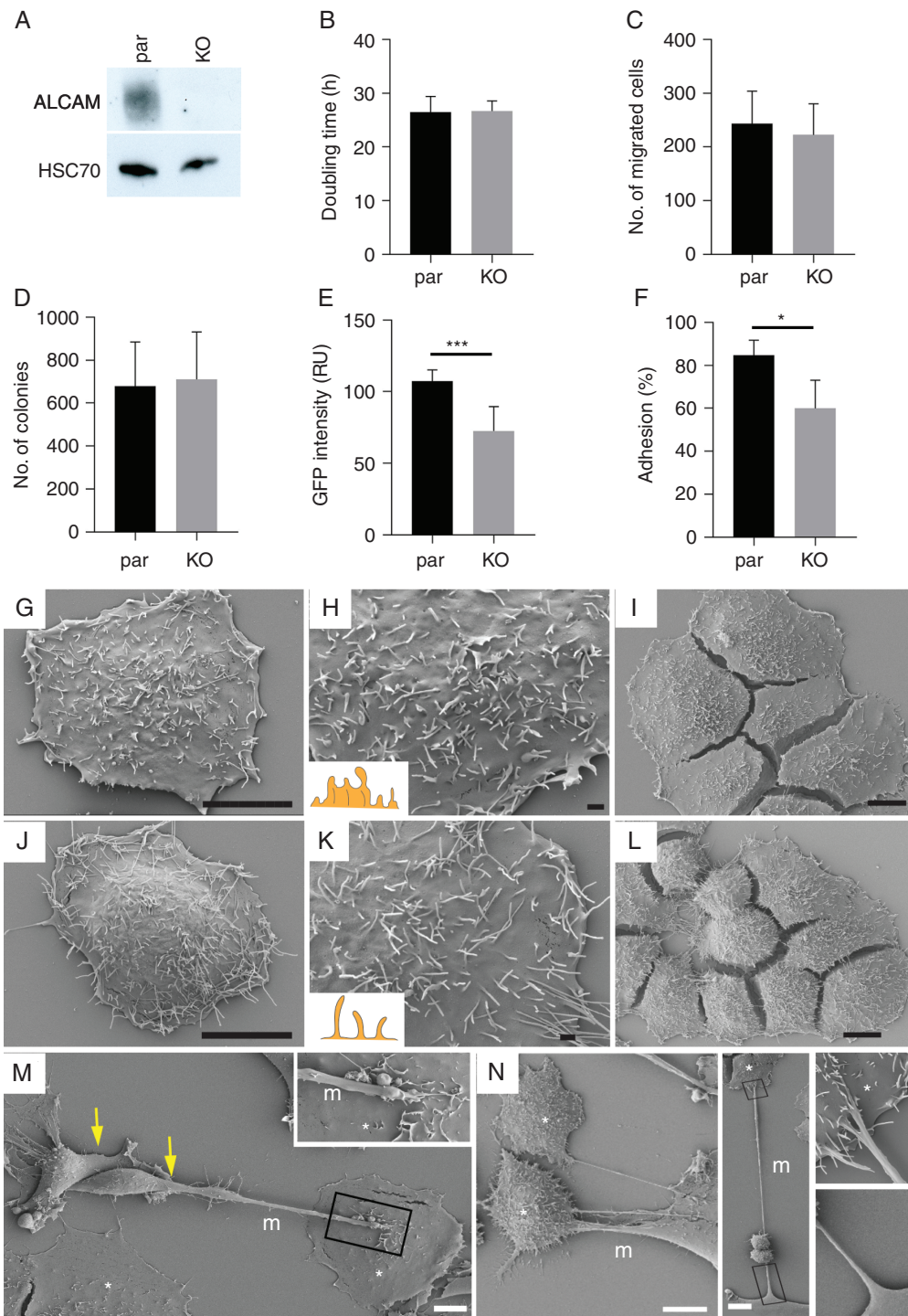
Fig. 3 Functional analyses of ALCAM in NSCLC cells. (A) Silencing of ALCAM in NCI-H460 cells by CRISPR/Cas ALCAM-KO was confirmed by immunoblot. Absence of ALCAM has no influence on proliferation (B, $P = 0.689$), migration (C, $P = 0.895$), and colony formation capacity (D, $P = 0.771$). Adhesion on hCMEC/D3 EC under static conditions was significantly reduced in H460 ALCAM-KO cells compared with parental cells (E, $P \leq 0.001$). (F) Adhesion after exposure to shear stress was significantly reduced in ALCAM-KO cells ($P = 0.045$). (G–N) Parental cancer H460 cells (G–I, M) and ALCAM KO counterparts (J–L, N) were cultured alone (G–L) or mixed (1:1) with EC (M, N), cultured for 2 days on gelatin-coated coverslips prior to processing for scanning electron microcopy. Insets show higher magnification of certain regions indicated with boxes (M, N). Drawings show the appearance of plasma membrane protrusions at their surface (H, K). Asterisk, cancer cells; arrow, EC; m, magnupod. Mean ± SD. Scale bars, 1 μm (H, K); 10 μm (G, I, J, L–N).
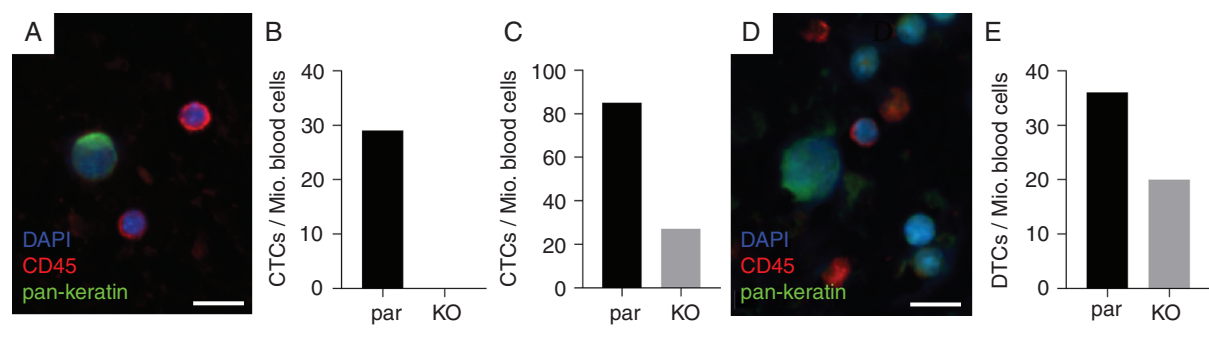
Fig. 4 Liquid biopsy and tumor outgrowth in intracranial and intracardial injected mice. (A–C) Liquid biopsy from injected mice showing no detectable CTCs in the blood of intracranial injected mice (B) and fewer CTCs in the blood of intracardially injected mice (C) when H460 ALCAM-KO cells were injected. Analysis of bone marrow aspirates shows fewer DTCs of H460 ALCAM-KO intracranially injected mice (E). Scale bars in A, D: 20 μm.

tumor growth could be found in the lateral ventricles of all mice injected with ALCAM-KO H460 cells, which was not observed in any of the parental H460 injected animals (0/5; Fig. 5C). Due to the location of the injection site (tracking of needle path), we believe that the cells were not injected in the ventricle, rather that the cells migrated there. To analyze whether the induced tumors are differentially vascularized, immunohistochemical staining for the endothelial cell adhesion molecule CD34 was performed with no difference observed between the 2 groups in terms of number, size, or form of vessels (Supplementary Fig. 2A–C). Finally, as bone is the most common site of metastases in cancer patients, we searched bone remodeling in the vertebral bodies and femur by sections and μCT, respectively. No signs of osteolytic lesions or bone remodeling, neither in spine nor in femora, assessed by μCT were observed (Supplementary Fig. 2E, F, I–L).

To assess the involvement of ALCAM in the dissemination to the brain, we performed intracardiac injection of parental and ALCAM-KO H460 cells. At time of sacrifice, mice injected with H460 parental cells had significantly more BM compared with ALCAM-KO injected mice (parental 24, range 16–45, ALCAM-KO 14, range 1–18, $P = 0.0004$; Fig. 5E, F, G) and showed a significantly higher total tumor load throughout the brain (parental 8.93, range 1.3–23.2 mm^3, ALCAM-KO 2.08, range 0.1–7.6 mm^3, $P = 0.0078$; Fig. 5H). None of the mice showed signs of metastasis in the ventricles. No differences in the form and number of blood vessels were found (Supplementary Fig. 2D). Similarly to the intracranial model, CTC analysis revealed 68% less CTCs per 1 million PBMCs in mice injected with H460 ALCAM-KO cells compared with H460 parental injected ones (parental 85 CTCs per 1 million PBMCs, ALCAM-KO 27 CTCs per 1 million PBMCs; Fig. 4C). Analysis of undecalcified vertebral body sections revealed metastases in the spine and femur of both groups, which was independent of ALCAM (Supplementary Fig. 2G, H, M–P). However, we could observe a decrease in bone mineral density of the femora in H460 parental injected mice (parental 793.3 ± 25.9, ALCAM-KO 828.4 ± 12.7; Supplementary Fig. 2Q).

Discussion

Cell adhesion is essential for cell communication and cell architecture. In tumor progression a change of cell architecture contributes to dissemination and metastasis.[18,32] ALCAM has previously been shown to be involved in tumor progression and metastasis,[18,33–35] but the potential impact of this protein on BM formation is currently unknown. In this study we analyzed the protein expression of ALCAM in primary tumors, CTCs, and BM and assessed its functional role in tumor dissemination, adhesion, and BM formation in in vitro and in vivo models.

In our analysis, ALCAM expression was found to be significantly elevated in BM compared with primary tumors. Specifically, in matched tissue an ALCAM upregulation from the primary tumors to BM in one third of cases was found, suggesting an important role in BM. Positive ALCAM status in primary NSCLC tumors has previously been linked to poor prognosis.[31] Here we show that it is particularly connected to NSCLC BM as well as to lymph node metastasis. Importantly, an elevated level of ALCAM expression in both the primary tissue and BM was associated with a shorter OS (both $P < 0.05$). In order to assess at which stage ALCAM upregulation might take place, matched CTCs and BM were analyzed for ALCAM expression. Although of clinical relevance, CTCs are rare in oligo-BM NSCLC[36] and therefore the ALCAM expression could be assessed in CTCs from only 4 patients. CTCs and BM samples showed in all cases a congruent ALCAM expression, suggesting that ALCAM expression of CTCs in the peripheral blood might represent the ALCAM status of the BM. However, further studies would need to be performed, especially on patients before they develop overt BM detectable by imaging in order to assess the CTCs with "true brain metastasis seed."

We further analyzed whether the secreted sALCAM form in blood serum could serve as an additional non-invasive biomarker. Secreted ALCAM is formed through shedding of its ectodomain by the metalloprotease ADAM17/TACE,[28] and high levels have been associated with a more
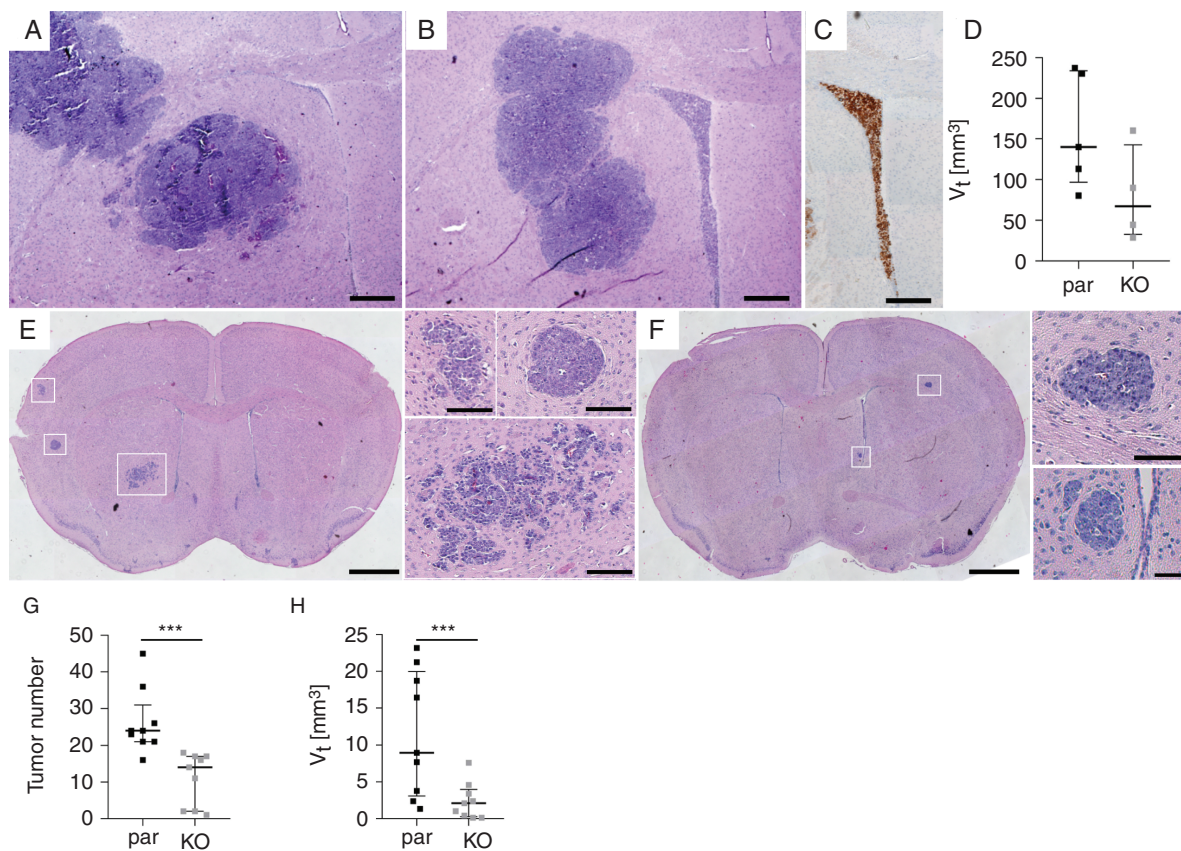
Fig. 5 (A, B, D) Tumor outgrowth was not significantly different between parental (A) and ALCAM-KO (B) intracranially injected mice (D, $P = 0.1905$). Tumor cells were detected in the lateral ventricle of ALCAM-KO intracranially injected mice (C, 4/4 injected mice), whereas in 0/5 of parental injected mice. (E, F). Representative pictures of whole brain sections from mice injected intracardially with either H460 parental (E) or H460 ALCAM-KO (F) cells showing number and size of tumors. Tumor number (G, $P = 0.0004$) and total tumor volume (H, $P = 0.0078$) is significantly higher in H460 parentally injected mice. Median ± interquartile range. Scale bars in A–C: 500 μm; in E, F: 1000 μm, in inserts of E, F: 100 μm.

aggressive tumor type in epithelial ovarian cancer.[36] We found sALCAM serum levels significantly elevated in multi-metastatic NSCLC patients compared with non-metastatic tumor patients and oligo-BM patients. As in other tumor entities, sALCAM might function as a general marker for dynamic tumor progression; in NSCLC it can be discussed as an overall prognostic factor not specifically linked to BM.[36–38]

Based on these observations we assumed that ALCAM expression might in particular affect BM formation of NSCLC cells. Hence we sought to test our hypothesis in an ALCAM-depleted NSCLC cell line model. ALCAM is known to promote cell migration associated with tumor progression and metastasis in other tumor entities.[34,39–42] Importantly, ALCAM has been shown to be crucial for leukocyte transendothelial migration through the BBB.[43–45] Our functional analysis of H460 ALCAM-depleted cells showed no changes in cell viability but a significant decrease in cell adhesion. By using both, a static assay and under flow condition mimicking the blood stream in microvessels, we showed that the adhesion capacity of ALCAM-depleted cells to brain endothelial cells was significantly reduced. This effect is similar to L1CAM, which promotes breast cancer BM formation by vascular

co-option of brain vascular endothelium.[20] We assume that ALCAM might be important for facilitating the extravasation of lung tumor cells through the BBB by mediating adhesion by both heterophilic (ALCAM-CD9) and homophilic (ALCAM-ALCAM) cell adhesion.[30,46] Brain ECs express high levels of ALCAM,[43] facilitating a strong cell contact between tumor cells expressing ALCAM and ECs. Further assessment using a scanning electron microscope showed an altered shape of ALCAM-depleted cells, indicating a cell architecture disruption and adhesion deficiency both at the apical (ruffles vs microvilli) and lateral (cell shape) sides of the cells. Although both cells (parental and ALCAM-KO) seem to interact with the brain ECs, a stronger contact is mediated through the ruffles in the parental cells, whereas ALCAM-KO cells were less strongly connected to the ECs via the microvilli. Interestingly, silencing ALCAM promoted an upregulation of its interacting partner CD9 that transforms the cellular morphology and eventually their migration. This hypothesis is supported by the study by Rappa et al, who showed that the knockdown of CD9 in breast cancer cells promoted the formation of membrane ruffles instead of microvilli.[47]

In order to assess if ALCAM is involved in both the tumor cell dissemination across the BBB as well as outgrowth in the brain, we used 2 different in vivo mouse models. We could show that intracardially injected H460 ALCAM-KO cells lead to fewer BM with less total tumor load compared with the parental cell line. In contrast, tumor outgrowth was unaffected by ALCAM status in the intracranial model. These data support our hypothesis that ALCAM is rather involved in tumor dissemination than metastatic outgrowth. Moreover, in the intracranial model, no CTCs could be detected in the mice injected with ALCAM-KO cells. Similarly, also the intracardial injection model showed a significant decrease (68%) in CTCs when ALCAM-KO cells were injected compared with parental cells. It has been shown that CTCs from primary brain tumors can exit the brain to the circulation.[48,49] This indicates that the BBB is not an unpassable barrier for CTCs. Accordingly, we identified fewer CTCs in the intracranial model of parental H460 ALCAM cells compared with the cardiac injection. The lack of CTCs in the intracranial ALCAM-KO model could indicate a problem in passing the BBB due to impaired adhesion of the tumor cells to brain endothelial cells, as shown by our in vitro data. However, the intracardiac model indicates that ALCAM might also give the tumor cells a survival advantage in the blood circulation. Thus, ALCAM might be involved in metastasis formation through different mechanisms.

We couldn't find any differences in either the vessel counts between the models indicating no significant impact of ALCAM on angiogenesis or in the formation of bone metastases. Obviously, these data of ALCAM-associated differential dissemination and metastatic patterns need to be verified using different models prospectively.

In summary, we demonstrated elevated ALCAM expression levels in human NSCLC BM. We showed that an ALCAM-positive status is correlated with poor outcome in lung cancer patients in both primary tumor setting as well as among brain metastatic patients. Further in vitro and in vivo findings support a role for ALCAM in brain dissemination and outgrowth, most likely via the interaction with brain ECs. Currently the first phase II trial is ongoing in which an ALCAM-directed probody drug conjugate is being tested on different primary cancer entities.[50] This emphasizes the potential clinical use of ALCAM as a novel therapeutic target. Our results suggest that in addition, ALCAM might represent a novel preventive target to reduce the occurrence of BM in NSCLC.

Supplementary Material

Supplementary data are available at *Neuro-Oncology* online.

Keywords

ALCAM adhesion | blood-brain barrier | NSCLC brain metastasis

Funding

Conflict of interest statement. None.

Acknowledgments

Authorship statement. Study concept and design: JM, DL, SW, MW, HW. Data analysis: JM, DL, SW, JK, MGa, MW, CM, HW. Patient sample collection: JM, KL, JMa, YV, GU, SSt, MGl. Performed experiments: JM, DL, LB, SW, JK, MGa, SS, KB, FH, JA, LO-F, CM. Data Interpretation: JM, DL, LB. MGa, AB, SWS, AKH, TS, DC, CM, HW. Drafted manuscript: JM, DL, SW, KP, HW. Approved final manuscript: all authors

References

1. Torre LA, Bray F, Siegel RL, Ferlay J, Lortet-Tieulent J, Jemal A. Global cancer statistics, 2012. *CA Cancer J Clin.* 2015; 65(2):87–108.

2. Malvezzi M, Bertuccio P, Rosso T, et al. European cancer mortality predictions for the year 2015: does lung cancer have the highest death rate in EU women? *Ann Oncol.* 2015;26(4):779–786.

3. Torre LA, Siegel RL, Jemal A. Lung cancer statistics. *Adv Exp Med Biol.* 2016;893:1–19.

4. Dawe DE, Greenspoon JN, Ellis PM. Brain metastases in non-small-cell lung cancer. *Clin Lung Cancer.* 2014;15(4):249–257.

5. Lassen U, Kristjansen PE, Hansen HH. Brain metastases in small-cell lung cancer. *Ann Oncol.* 1995;6(9):941–944.

6. Villano JL, Durbin EB, Normandeau C, Thakkar JP, Moirangthem V, Davis FG. Incidence of brain metastasis at initial presentation of lung cancer. *Neuro Oncol.* 2015;17(1):122–128.

7. Hu C, Chang EL, Hassenbusch SJ 3rd, et al. Nonsmall cell lung cancer presenting with synchronous solitary brain metastasis. *Cancer.* 2006;106(9):1998–2004.

8. Hall WA, Djalilian HR, Nussbaum ES, Cho KH. Long-term survival with metastatic cancer to the brain. *Med Oncol.* 2000;17(4):279–286.

9. Ali A, Goffin JR, Arnold A, Ellis PM. Survival of patients with non-small-cell lung cancer after a diagnosis of brain metastases. *Curr Oncol.* 2013;20(4):e300–e306.

10. Chamberlain MC, Baik CS, Gadi VK, Bhatia S, Chow LQ. Systemic therapy of brain metastases: non-small cell lung cancer, breast cancer, and melanoma. *Neuro Oncol.* 2017;19(1):i1–i24.

11. Zlokovic BV. The blood-brain barrier in health and chronic neurodegenerative disorders. *Neuron.* 2008;57(2):178–201.

12. Daneman R. The blood-brain barrier in health and disease. *Ann Neurol.* 2012;72(5):648–672.

13. Ramakrishna R, Rostomily R. Seed, soil, and beyond: the basic biology of brain metastasis. *Surg Neurol Int.* 2013;4(Suppl 4):S256–S264.

14. Witzel I, Oliveira-Ferrer L, Pantel K, Müller V, Wikman H. Breast cancer brain metastases: biology and new clinical perspectives. *Breast Cancer Res.* 2016;18(1):8.

15. Hanssen A, Wagner J, Gorges TM, et al. Characterization of different CTC subpopulations in non-small cell lung cancer. *Sci Rep.* 2016;6:28010.

16. Boral D, Vishnoi M, Liu HN, et al. Molecular characterization of breast cancer CTCs associated with brain metastasis. *Nat Commun.* 2017;8(1):196.

17. Hanssen A, Loges S, Pantel K, Wikman H. Detection of circulating tumor cells in non-small cell lung cancer. *Front Oncol.* 2015;5:207.

18. Wai Wong C, Dye DE, Coombe DR. The role of immunoglobulin superfamily cell adhesion molecules in cancer metastasis. *Int J Cell Biol.* 2012;2012:340296.

19. Beauchemin N, Arabzadeh A. Carcinoembryonic antigen-related cell adhesion molecules (CEACAMs) in cancer progression and metastasis. *Cancer Metastasis Rev.* 2013;32(3-4):643–671.

20. Valiente M, Obenauf AC, Jin X, et al. Serpins promote cancer cell survival and vascular co-option in brain metastasis. *Cell.* 2014;156(5):1002–1016.

21. Kienast Y, von Baumgarten L, Fuhrmann M, et al. Real-time imaging reveals the single steps of brain metastasis formation. *Nat Med.* 2010;16(1):116–122.

22. Wilhelm I, Molnár J, Fazakas C, Haskó J, Krizbai IA. Role of the blood-brain barrier in the formation of brain metastases. *Int J Mol Sci.* 2013;14(1):1383–1411.

23. Brayton J, Qing Z, Hart MN, VanGilder JC, Fabry Z. Influence of adhesion molecule expression by human brain microvessel endothelium on cancer cell adhesion. *J Neuroimmunol.* 1998;89(1-2):104–112.

24. Soto MS, Serres S, Anthony DC, Sibson NR. Functional role of endothelial adhesion molecules in the early stages of brain metastasis. *Neuro Oncol.* 2014;16(4):540–551.

25. Hvichia GE, Parveen Z, Wagner C, et al. A novel microfluidic platform for size and deformability based separation and the subsequent molecular characterization of viable circulating tumor cells. *Int J Cancer.* 2016;138(12):2894–2904.

26. Kunkel P, Ulbricht U, Bohlen P, et al. Inhibition of glioma angiogenesis and growth in vivo by systemic treatment with a monoclonal antibody against vascular endothelial growth factor receptor-2. *Cancer Res.* 2001;61(18):6624–6628.

27. Koch C, Joosse SA, Schneegans S, et al. Pre-analytical and analytical variables of label-independent enrichment and automated detection of circulating tumor cells in cancer patients (submitted).

28. Rosso O, Piazza T, Bongarzone I, et al. The ALCAM shedding by the metalloprotease ADAM17/TACE is involved in motility of ovarian carcinoma cells. *Mol Cancer Res.* 2007;5(12):1246–1253.

29. Kalagara T, Moutsis T, Yang Y, et al. The endothelial glycocalyx anchors von Willebrand factor fibers to the vascular endothelium. *Blood Adv.* 2018;2(18):2347–2357.

30. Gilsanz A, Sánchez-Martín L, Gutiérrez-López MD, et al. ALCAM/CD166 adhesive function is regulated by the tetraspanin CD9. *Cell Mol Life Sci.* 2013;70(3):475–493.

31. von Lersner A, Droesen L, Zijlstra A. Modulation of cell adhesion and migration through regulation of the immunoglobulin superfamily member ALCAM/CD166. *Clin Exp Metastasis.* 2019;36(2):87–95.

32. Raz A, Ben-Ze'ev A. Cell-contact and -architecture of malignant cells and their relationship to metastasis. *Cancer Metastasis Rev.* 1987;6(1):3–21.

33. Ishiguro F, Murakami H, Mizuno T, et al. Membranous expression of activated leukocyte cell adhesion molecule contributes to poor prognosis and malignant phenotypes of non-small-cell lung cancer. *J Surg Res.* 2013;179(1):24–32.

34. Devis L, Moiola CP, Masia N, et al. Activated leukocyte cell adhesion molecule (ALCAM) is a marker of recurrence and promotes cell migration, invasion, and metastasis in early-stage endometrioid endometrial cancer. *J Pathol.* 2017;241(4):475–487.

35. Ofori-Acquah SF, King JA. Activated leukocyte cell adhesion molecule: a new paradox in cancer. *Transl Res.* 2008;151(3):122–128.

36. Carbotti G, Orengo AM, Mezzanzanica D, et al. Activated leukocyte cell adhesion molecule soluble form: a potential biomarker of epithelial ovarian cancer is increased in type II tumors. *Int J Cancer.* 2013;132(11):2597–2605.

37. Tachezy M, Effenberger K, Zander H, et al. ALCAM (CD166) expression and serum levels are markers for poor survival of esophageal cancer patients. *Int J Cancer.* 2012;131(2):396–405.

38. Arnold Egloff SA, Du L, Loomans HA, et al. Shed urinary ALCAM is an independent prognostic biomarker of three-year overall survival after cystectomy in patients with bladder cancer. *Oncotarget.* 2017;8(1):722–741.

39. Weidle UH, Eggle D, Klostermann S, Swart GW. ALCAM/CD166: cancer-related issues. *Cancer Genomics Proteomics.* 2010;7(5):231–243.

40. Ishiguro F, Murakami H, Mizuno T, et al. Activated leukocyte cell-adhesion molecule (ALCAM) promotes malignant phenotypes of malignant mesothelioma. *J Thorac Oncol.* 2012;7(5):890–899.

41. Lunter PC, van Kilsdonk JW, van Beek H, et al. Activated leukocyte cell adhesion molecule (ALCAM/CD166/MEMD), a novel actor in invasive growth, controls matrix metalloproteinase activity. *Cancer Res.* 2005;65(19):8801–8808.

42. Degen WG, van Kempen LC, Gijzen EG, et al. MEMD, a new cell adhesion molecule in metastasizing human melanoma cell lines, is identical to ALCAM (activated leukocyte cell adhesion molecule). *Am J Pathol.* 1998;152(3):805–813.

43. Cayrol R, Wosik K, Berard JL, et al. Activated leukocyte cell adhesion molecule promotes leukocyte trafficking into the central nervous system. *Nat Immunol.* 2008;9(2):137–145.

44. Masedunskas A, King JA, Tan F, et al. Activated leukocyte cell adhesion molecule is a component of the endothelial junction involved in transendothelial monocyte migration. *FEBS Lett.* 2006;580(11):2637–2645.

45. Bowen MA, Patel DD, Li X, et al. Cloning, mapping, and characterization of activated leukocyte-cell adhesion molecule (ALCAM), a CD6 ligand. *J Exp Med.* 1995;181(6):2213–2220.

46. van Kempen LC, Nelissen JM, Degen WG, et al. Molecular basis for the homophilic activated leukocyte cell adhesion molecule (ALCAM)-ALCAM interaction. *J Biol Chem.* 2001;276(28):25783–25790.

47. Rappa G, Green TM, Karbanová J, Corbeil D, Lorico A. Tetraspanin CD9 determines invasiveness and tumorigenicity of human breast cancer cells. *Oncotarget.* 2015;6(10):7970–7991.

48. Muller C, Holtschmidt J, Auer M, et al. Hematogenous dissemination of glioblastoma multiforme. *Sci Transl Med.* 2014;6(247):247ra101.

49. Sullivan JP, Nahed BV, Madden MW, et al. Brain tumor cells in circulation are enriched for mesenchymal gene expression. *Cancer Discov.* 2014;4(11):1299–1309.

50. ClinicalTrials.gov. PROCLAIM-CX-2009: a trial to find safe and active doses of an investigational drug CX-2009 for patients with selected solid tumors. 2017; NCT03149549. Available at: https://clinicaltrials.gov/ct2/show/study/NCT03149549?term=CD166&rank=4. Accessed July 19, 2019.